

Effective masses in $\text{In}_{1-x}\text{Ga}_x\text{As}$ superlattices derived from Franz-Keldysh oscillations

B. Schlichtherle and G. Weiser

Department of Physics and Center of Material Sciences, University of Marburg, D-35032 Marburg, Germany

M. Klenk

Alcatel SEL AG, Research Center, Lorenzstraße 10, D-70435 Stuttgart, Germany

F. Mollot and Ch. Starck

Alcatel Alsthom Recherche, Route de Nozay, F-91460 Marcoussis, France

(Received 12 June 1995)

$\text{In}_{1-x}\text{Ga}_x\text{As}$ superlattices with InP or $\text{In}_{1-x}\text{Ga}_x\text{As}_y\text{P}_{1-y}$ barriers show in small fields, below the onset of Stark localization, Franz-Keldysh oscillations that give direct access to the miniband mass. The mass at the bottom of the first miniband is similar to that of the wells. A second set of oscillations is observed at the saddle-point edge, which points to a smaller mass on top of the first miniband. A very small mass, $0.014m_0$, is obtained for the minimum of the second miniband. Stark localization in this band is not observed, most likely due to efficient tunneling into higher bands.

Quantum-well superlattices provide a class of semiconductors whose bandwidth Δ varies with height and thickness of the barrier. Kronig-Penney models in tight binding approximation predict different masses for minibands emerging from different sublevels of the quantum well, which depend only on bandwidth and period a of the superlattice:¹

$$m_{s1} = \frac{2}{\Delta} \left(\frac{\hbar}{a} \right)^2. \quad (1)$$

The Franz-Keldysh effect measured with electric fields in growth direction provides direct access to the miniband mass. The field alters the density of states, resulting above the energy gap E_g in characteristic oscillations of the field induced change $\Delta\alpha$ of the absorption constant. The line shape of the $\Delta\alpha$ spectrum scales with field strength F and the reduced mass m^* in field direction leading to a simple relation of index number n and energy E_n of its peaks:²

$$(E_n - E_g)^{3/2} = \frac{3e\hbar F}{8\sqrt{2m^*}} n. \quad (2)$$

The method has been applied to bulk semiconductors with large Brillouin zones and wide bands to determine the mass² or the field in heterostructures.³ In a superlattice, however, electrons can be accelerated to the edge of the much smaller Brillouin zone before scattering occurs. Bragg reflection leads to new boundary conditions that perturb the simple sequence of Franz-Keldysh oscillations, resulting finally in Stark localization.⁴ Observation of unperturbed Franz-Keldysh oscillations in a miniband therefore requires small fields to prevent carriers from reaching the edge of the Brillouin zone and the top of the miniband. If L is the mean free path, the upper limit of the field is estimated to

$$F_{\max} = \Delta/eL, \quad (3)$$

which for a typical bandwidth of 60 meV and a mean free path of 100 nm restricts the field to less than 10 kV/cm. The useful range of fields is small because the field should be large enough to overcome Coulombic effects that distort the line shape near the absorption edge.⁵ Previous studies on GaAs superlattices used relatively large fields^{6,7} and evaluated only the width of the features at the absorption edge.⁸

Results from two superlattices grown lattice matched on n -InP will be presented. Sample A consists of 36 $\text{In}_{1-x}\text{Ga}_x\text{As}$ wells, 4.5 nm thick with 2.7-nm-thin InP barriers, embedded between 120-nm-thick undoped InP layers, resulting in a thickness of undoped material of 0.5 μm . Kronig-Penney calculations yield 63-meV-wide miniband. The light hole bandwidth was calculated to 22 meV, while that of the heavy hole band was negligible (0.1 meV). Sample B had 100 $\text{In}_{1-x}\text{Ga}_x\text{As}$ quantum wells, 8.2 nm wide with 3.2-nm-thin barriers of $\text{In}_{1-x}\text{Ga}_x\text{As}_y\text{P}_{1-y}$ of a low-temperature gap at 1.13 eV. The wide wells accommodate two electron sublevels resulting in 34- and 125-meV-wide minibands. Heavy hole bands again were negligibly small. Superlattice B was placed between 150-nm-thick quaternary layers increasing the total thickness of the undoped regions to 1.44 μm . Both stacks were capped with a p -type InP cap layer and coated with a 5-nm-thin transparent Pt electrode. The substrate served as a counter electrode. The internal field arising from the diffusion potential is changed by dc bias while a small modulating voltage alters the transmitted intensity $\Delta I/I = -d\Delta\alpha$, where d is the thickness of the superlattice. All measurements were performed at 15 K in a setup described before.³

Figure 1 compares absorption and electroabsorption spectra of sample A for different fields. Absorption peaks reveal Stark localization even under zero bias. The peaks belong to intrawell ($\nu = 0$) and first-order Stark ladder transitions ($\nu = \pm 1$). Their separation corresponds to a built-in field of 26 kV/cm in accordance with a diffusion potential of 1.3 V. The electroabsorption spectrum

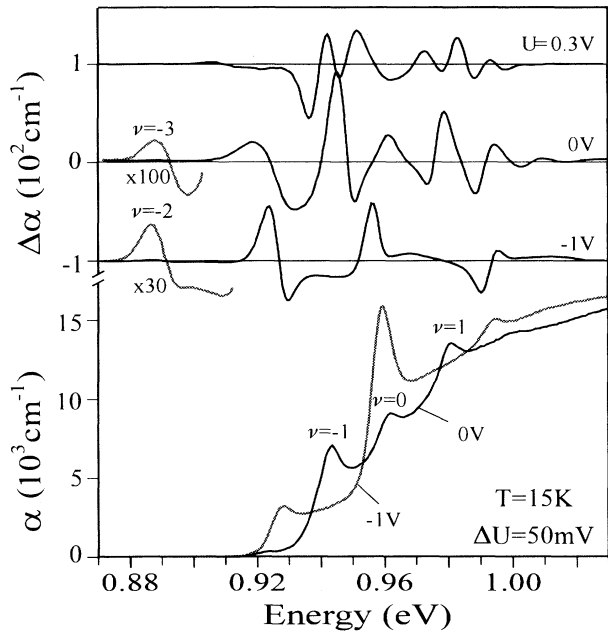


FIG. 1. Sample A, comparison of absorption and electroabsorption spectra for different bias voltage. Small spectral features are enlarged by the indicated factors.

shows a complicated structure and resolves weak transitions over three barriers ($\nu = -3$). The absorption spectrum under reverse bias (-1 V) is dominated by strong intrawell transitions, which acquired strength at the expense of the Stark ladder transitions. This increasing strength leads to a positive peak in the center of the $\Delta\alpha$ spectrum while the line shape of Stark ladder transitions is determined by their field induced shift.⁹ Under forward bias, the $\Delta\alpha$ spectrum changes to a manifold of peaks, occurring mainly on the edges of the miniband, and weak higher-order Stark ladder transitions split off at low energy. The shift of the Stark ladder transitions shows that increasing the reverse bias by 1 V increases the field by 18.5 kV/cm, indicating little screening by space charge at the interfaces to doped regions. Above 0.5 V, forward bias carriers diffusing into the intrinsic region cause partial screening of the applied voltage apparent in a smaller signal height. It also slows down the reduction of the field by forward bias to about half the rate observed for reverse bias.

Reduction of the field is limited to 1.3 V forward bias to avoid electroluminescence in phase with the modulating voltage. A smooth absorption spectrum indicates that excitons of the miniband are still ionized by the field. This field, estimated to 7 ± 1 kV/cm, is sufficiently small to observe Franz-Keldysh oscillations over the whole range of the electron miniband (Fig. 2). Oscillations starting from the M_0 singularity at the bottom of the band extend, slowly decreasing in strength, to the top where they overlap with a second set of broader oscillations starting at the M_1 saddle point in perfect agreement with the anticipated line shape.¹⁰ In a field of 7 kV/cm, carriers reach the upper band edge after traveling 90 nm, which is less than the size of coherent states derived from

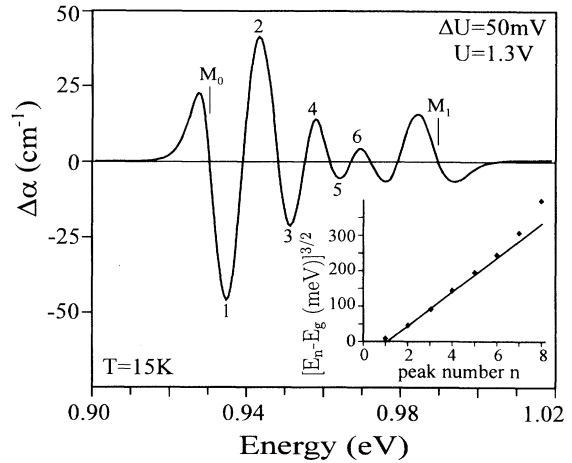


FIG. 2. Sample A, electroabsorption spectrum at low field. The inset proves that peak positions obey the relation for Franz-Keldysh oscillations.

the Franz-Keldysh effect in bulk $\text{In}_{1-x}\text{Ga}_x\text{As}$ (160 nm).¹¹ The overlap suggests indeed the onset of Stark localization as Bragg reflection reduces coherent states to a size smaller than given by scattering processes. However, for most of the spectrum the overlap is small and the first six peaks obey Eq. (2) identifying them as Franz-Keldysh oscillations (inset Fig. 2). For the estimated field a reduced mass of $0.045 \pm 0.012 m_0$ is obtained, which is the electron mass due to negligible dispersion of the heavy hole band. The mass agrees with the value $0.046 m_0$ predicted from the bandwidth in a Kronig-Penney model and is close to the mass of the well material ($0.041 m_0$). Although the accuracy is limited by the uncertainty of the field, the result confirms a small anisotropy of the first electron miniband as suggested from luminescence data in magnetic fields.¹² The larger separation of the remaining peaks evolving from the saddle point M_1 points to a significantly smaller mass on top of the first miniband but more oscillations must be resolved to confirm the value $0.025 m_0$ evaluated from the width of the leading features.

A small built-in field was expected in the thicker superlattice B. However, the field turned out to be inhomogeneous due to carriers diffusing into the superlattice,¹³ which caused also partial screening of the external voltage up to a reverse bias voltage of 2 V. Above this threshold the field increased by 6.5 kV/cm for 1-V bias, which is close to the value 7 kV/cm, the ratio of external voltage and thickness of undoped material. This rate is the same in the superlattice, obtained from the shift of third-order Stark ladder transitions, and in the quaternary cladding layers, derived from Franz-Keldysh oscillations above their gap at 1.13 eV. Figure 3 compares absorption and electroabsorption spectra at a field of about 12–14 kV/cm, large enough to localize the electrons in the first miniband to a few unit cells in accordance with the weak response of the third-order Stark ladder transitions at 817 meV in the $\Delta\alpha$ spectrum. The first steep edge of the absorption spectrum, which again shows no excitonic fine

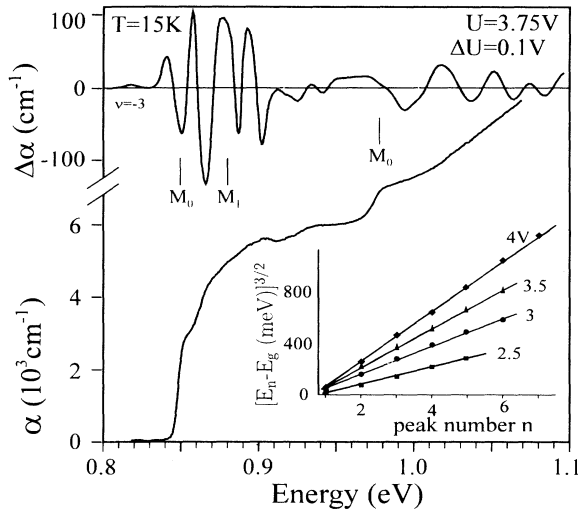


FIG. 3. Sample B, comparison of absorption and electroabsorption spectra under small reverse bias. The inset displays the Franz-Keldysh fan of oscillations of the second miniband.

structure, is due to transitions from heavy hole states, followed about 25 meV later by the weaker excitations of light holes. All strong features of the $\Delta\alpha$ spectrum are attributed to heavy hole states because light hole transitions in similar quantum wells have been found to respond only weakly to the field.⁹ M_0 and M_1 give the calculated transition energies from the heavy hole state to the singularities of the electron miniband. The oscillations of $\Delta\alpha$ at the absorption edge extend far beyond this bandwidth. They cannot be attributed to the Franz-Keldysh effect of the first miniband but reflect the redistribution of oscillator strength among Stark ladder transitions similar as observed in photocurrent spectra in a GaAs superlattice.¹⁴

The minimum M_0 of the second, 125-meV-wide electron miniband is almost degenerate with the bottom of the conduction band of the barrier material. The absorption spectrum shows at the expected position (0.975 eV) a second smaller edge attributed to transitions into this band from the narrow second heavy hole band (0.6 meV). The $\Delta\alpha$ spectrum shows there a set of oscillations which, as shown in Fig. 4, broaden rapidly with increasing reverse bias in perfect agreement with Eq. (2) for Franz-Keldysh oscillations (inset in Fig. 3). The evaluation yields for a field of 12 kV/cm a mass of only $0.012m_0$.

Because of some uncertainty of the field strength, we control the field by evaluating also the linear relation of field in the superlattice determined from the Franz-Keldysh oscillations and external bias. (Shown as inset in Fig. 4.) Franz-Keldysh oscillations yield the ratio F/\sqrt{m} . For the fields in the inset, we used a mass $0.041m_0$, the electron mass in $\text{In}_{1-x}\text{Ga}_x\text{As}$. Fields based on this mass correspond to an increase of the field by 12 kV/cm for 1 V increase of the bias voltage. This rate is almost twice as large as that obtained from Stark ladder transitions of the first miniband and from

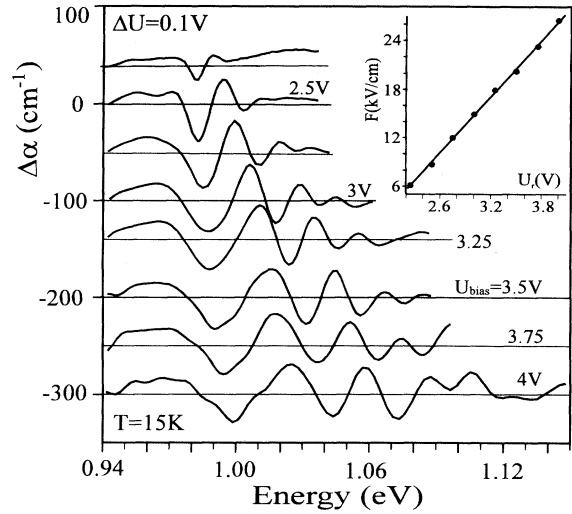


FIG. 4. Variation of Franz-Keldysh oscillations of the second miniband with reverse bias. The inset shows the linear relation of bias voltage and field derived from the oscillations assuming a mass of $0.041m_0$.

the Franz-Keldysh oscillations of the quaternary layers, which proves that the mass of the second miniband must be smaller than $0.041m_0$. Adjusting the change of the field to its maximum rate 7 kV/cm, the ratio of external voltage change and thickness of undoped material, yields the value $0.014m_0$ confirming the very small mass of the second miniband.

A similar reduction of the mass in a second miniband has been reported from luminescence excitation spectra in magnetic fields for a GaAs/ $\text{Al}_x\text{Ga}_{1-x}\text{As}$ superlattice¹² and to a smaller degree from interband magnetoabsorption of a $\text{In}_{1-x}\text{Ga}_x\text{As}/\text{In}_{1-x}\text{Ga}_x\text{As}_y\text{P}_{1-y}$ superlattice with wider barriers.¹⁵ These experiments involve also in-plane motion and extract the superlattice mass by evaluating the transition energies in a magnetic field, which introduces also some uncertainty while electroabsorption involves only the mass along the field and give therefore direct access to the miniband mass. A different mass at the minimum of the second miniband is also anticipated from its location in the Brillouin zone. The minimum of the second and the saddle point of the first miniband form a gap at the edge of the superlattice Brillouin zone. The gap and the curvature of the bands are related to the corresponding component of the superlattice potential. The small mass of the second miniband therefore is consistent with the smaller mass at the saddle point of the first miniband conjectured from the width of its Franz-Keldysh oscillations.

The small mass has led us to propose faster devices that employ transport in the second miniband.¹⁶ The advantage of a small mass could be compensated by rapid scattering into the lower lying first miniband. In striking contrast to Stark localization in the first miniband, which is observed already under forward bias conditions, the Franz-Keldysh oscillations of the second miniband are well defined under reverse bias and show no distortion by

Stark localization and Bragg reflection even for fields of 20 kV/cm, where electrons have to travel less than 7 nm to reach the top of the second miniband. This may point to fast electron scattering in the second miniband. Alternatively, electrons may tunnel into higher bands, which reduces the probability for Bragg reflection. Because the Franz-Keldysh oscillations are well defined and stretch over most of the miniband width, we consider tunneling as the likely reason for the absence of Stark localization in the second miniband.

In summary, we have demonstrated that Franz-Keldysh oscillations provide direct access to the effective mass of electron minibands in superlattices with an accuracy limited only by the knowledge of the field. The range of useful fields is quite limited because the field must be small enough to avoid Stark localization but large enough

to overcome excitonic effects and broadening by scattering processes. Wide neutral bulk layers should separate the superlattice from contact regions to reduce carrier diffusion into the superlattice and to establish small homogeneous fields. Under those conditions more Franz-Keldysh oscillations from the saddle-point edge, which in bulk material have never been observed, should be resolvable and the evaluation of the saddle-point mass will be improved. The small masses observed at the edge of the Brillouin zone are expected to depend strongly on the superlattice potential. Stark localization in the second miniband has not been observed, which is attributed to tunneling into higher bands.

This work has been supported by the European Community under Contract No. RACE 2006.

¹ L. Esaki and R. Tsu, *IBM J. Res. Dev.* **14**, 61 (1970).

² D. E. Aspnes, *Phys. Rev. Lett.* **31**, 230 (1973).

³ K. Satzke, H. G. Vestner, G. Weiser, L. Goldstein, and A. Perales, *J. Appl. Phys.* **69**, 7703 (1991).

⁴ J. Bleuse, G. Bastard, and P. Voisin, *Phys. Rev. Lett.* **60**, 220 (1988).

⁵ D. F. Blossey, *Phys. Rev. B* **2**, 3976 (1970).

⁶ F. Cerdeira, C. Vázquez-López, E. Ribeiro, P. A. M. Rodrigues, V. Lemos, M. A. Sacilotti, and A. P. Roth, *Phys. Rev. B* **42**, 9480 (1990).

⁷ C. Coriasso, D. Campi, C. Cacciato, C. Alibert, S. Gailard, B. Lambert, and A. Regreny, *Europhys. Lett.* **16**, 591 (1991).

⁸ H. Schneider, A. Fischer, and K. Ploog, *Phys. Rev. B* **45**, 6329 (1992).

⁹ G. Weiser, K. Satzke, B. Schlichterle, L. Goldstein, and A. Perales, *Phys. Rev. B* **45**, 14376 (1992).

¹⁰ D. E. Aspnes, *Phys. Rev.* **147**, 554 (1966).

¹¹ A. Jaeger and G. Weiser, *Proceedings of the IEEE Conference on Lasers and Electro-Optics, 7th Meeting, Boston, 1994* (IEEE, Piscataway, NJ, 1994), Vol. 2, p. 216.

¹² N. J. Pulsford and K. Ploog, *Surf. Sci.* **267**, 445 (1992).

¹³ H. T. Grahn, H. Schneider, and K. v. Klitzing, *Phys. Rev. B* **41**, 2890 (1990).

¹⁴ N. Linder, W. Geisselbrecht, G. Philipp, K. H. Schmidt, and G. Döhler, *J. Phys. (France) IV* **3**, 195 (1993).

¹⁵ S. L. Wong, R. J. Nicholas, C. G. Cureton, J. M. Jowett, and E. J. Thrush, *Semicond. Sci. Technol.* **7**, 493 (1992).

¹⁶ D. C. Herbert, *Semicond. Sci. Technol.* **3**, 101 (1988).